$$J(L) = -\beta\left(\frac{k}{6(2L+1)d^6} + \frac{g(L)k^3}{16d^4} + \frac{3h(L)k^5}{d^2} - 20w(L)k^7 \ln|2kd| + O(k^7)\right), \quad \text{(B5)}$$

where

$$g(L) = [(L+\tfrac{3}{2})(L+\tfrac{1}{2})(L-\tfrac{1}{2})]^{-1}, \quad \text{(B6)}$$

$$h(L) = [(2L+5)(2L+3)(2L+1)(2L-1)(2L-3)]^{-1}, \quad \text{(B7)}$$

and $w(L)$ is defined by (A3).

APPENDIX C: EVALUATION OF $K(L)$

In order to evaluate the integral $K(L)$, we insert (17) in (14) and make the substitution $z = kr$, which gives

$$K(L) = \tfrac{1}{2}\pi\beta k^7 \int_{kd}^{\infty} z^{-7}[J^2_{L+1/2}(z) + J^2_{-L-1/2}(z)]\,dz . \quad \text{(C1)}$$

The integral in (C1) may be evaluated using Eq. 9.62-5 of Ref. 13. We find

$$K(L) = -\frac{\beta}{d^7}\sum_{m=0}^{L}\frac{c_{Lm}}{2m-2L-7}(kd)^{2m-2L}, \quad \text{(C2)}$$

where the coefficients c_{Lm} are given by

$$c_{Lm} = \frac{2^{2m-2L}(2L-m)!(2L-2m)!}{[(L-m)!]^2 m!} . \quad \text{(C3)}$$

We note that Eq. (C2) holds for all values of L.

*Address until 15 December 1972: University of Florida, Gainesville, Fla. 32601.

[1]C. H. Page, Phys. Rev. 53, 426 (1938).
[2]G. Das and A. C. Wahl, Phys. Rev. A 4, 825 (1971).
[3]R. W. La Bahn and J. Callaway, Phys. Rev. 180, 91 (1969).
[4]M. H. Mittleman, Ann. Phys. (N.Y.) 14, 94 (1961).
[5]C. J. Kleinman, Y. Hahn, and L. Spruch, Phys. Rev. 165, 53 (1968).
[6]H. A. Bethe, Phys. Rev. 76, 38 (1949).
[7]B. R. Levy and J. B. Keller, J. Math. Phys. 4, 54 (1963).
[8]T. F. O'Malley, L. Spruch, and L. Rosenberg, J. Math. Phys. 2, 491 (1961).
[9]O. Hinckelmann and L. Spruch, Phys. Rev. A 3, 642 (1971).
[10]P. S. Ganas, Phys. Rev. A 5, 1684 (1972).
[11]E. Gerjuoy and S. Stein, Phys. Rev. 97, 1671 (1955).
[12]I. S. Gradshteyn and I. M. Ryzhik, *Tables of Integrals, Series and Products* (Academic, New York, 1965).
[13]G. N. Watson, *Theory of Bessel Functions* (Cambridge U. P., London, 1966).
[14]*Handbook of Mathematical Functions*, edited by M. Abramowitz and I. A. Stegun (Dover, New York, 1965).

PHYSICAL REVIEW A VOLUME 6, NUMBER 4 OCTOBER 1972

Absolute Cross Sections for Excitation of Neon by Impact of 20–180-keV H^+, H_2^+, and He^+ †

G. W. York, Jr.,* J. T. Park, V. Pol, and D. H. Crandall*
Physics Department, University of Missouri-Rolla, Rolla, Missouri 65401

(Received 12 April 1972)

The technique of heavy-ion energy-loss spectrometry has been used to measure excitation cross sections for the $(2p^5)3s$ and $(2p^5)3p$ electronic configurations of neon by impact of heavy ions upon ground-state neon. The incident particles used were H^+, H_2^+, and He^+ at impact energies from 20 to 180 keV. The results are compared with previous optical measurements of the emission cross sections of lines from these levels as excited by H^+ and He^+ impact. Agreement is not good, neither in shape nor in absolute magnitude, for excitation of the $(2p^5)3s$ configuration. However, agreement is surprisingly good for excitation of the $(2p^5)3p$ configuration. A curve-fitting technique has been applied to extract relative singlet-triplet cross sections for levels within the $(2p^5)3s$ configuration. Almost no triplet excitation is observed for H^+ and H_2^+ impact. Significant triplet excitation is observed only for He^+ impact.

I. INTRODUCTION

There has been considerable recent interest in the properties of neon as embodied in collision cross sections. Investigations have been conducted by bombarding neon with low-energy ions[1–3] and with electrons at energies ranging from threshold to several hundreds of eV.[4,5]

The extensive work of Coffey *et al.*[3] on inelastic and elastic scattering of He^+ by Ne at energies below 500 eV has indicated the wealth of information obtainable by collision spectroscopy. In this low-energy range, the observed patterns in the data can be explained quite reasonably in terms of molecular curve crossings which, in turn, yield valuable information concerning the nature of inter-

atomic forces. However, at energies in the keV range, the simple curve crossings do not explain the observed phenomena[3] and hence probably do not provide the dominant mechanism for inelastic processes in this energy range.

To date, very little emphasis has been placed on the acquisition of data which would help in our understanding of these processes. Among the few reported experimental efforts in this area are the works of de Heer and co-workers,[6,7] van Eck *et al.*,[8] and Jaecks *et al.*,[9] who have measured emission cross sections for spectral lines of neon induced by proton and He^+ impacts at energies up to 35 keV. Thomas and Gilbody[10] have bombarded the noble gases with high-energy (100–400-keV) helium ions but were not able to observe emission corresponding to excitation of atomic neon lines.

We have attempted to fill this gap in our knowledge by measuring cross sections for excitation of the two lowest electronic configurations of neon by impact of H, H_2, and He ions using the technique of heavy-ion energy-loss spectrometry.[11] The results presented cover the energy range 20–180 keV and are, to the authors' knowledge, the first measurements of the absolute cross sections for excitation of neon in this energy range.

The properties of neon are of interest because of the use of neon in lasers, as a possible charge-transfer agent for neutral injection into controlled thermonuclear plasmas,[12] and because of its deviation from Russell-Saunders (LS) coupling.[13]

II. EXPERIMENTAL

The apparatus and philosophy of heavy-ion energy-loss spectrometry have been discussed in detail elsewhere.[11] The following is a brief description of the apparatus, together with a more complete description of the angular acceptance of the apparatus. The latter is required since neon is more massive than previous targets.

Ions produced in a Colutron[14] low-voltage discharge source are accelerated and steered into a target chamber containing the gas under study. After traversing the scattering chamber, the forward-scattered beam is magnetically momentum analyzed to obtain the particular ion species of interest. This beam is then decelerated to a low well-defined energy and energy analyzed by a 127° electrostatic analyzer. Detection is accomplished by an 18-stage EMI electron multiplier. Target density is monitored by an MKS Baratron[15] differential-pressure meter, which is taken as the laboratory standard.

Spectra differential in energy loss are obtained by slowly increasing the potential difference between the accelerator and decelerator terminals. Whenever the increased potential difference compensates for a discrete energy loss of the projectile-target system, a peak is detected in the spectrum. It should be noted that the technique of compensating for the energy lost in the collision ensures that all detected particles have traversed similar trajectories through the mass and energy analyses and the deceleration column. Thus, cross sections obtained with this device are absolute to the extent that they are independent of relative detection efficiency.

Recent modifications[16] have been made which have permitted determination of the energy-loss scale to an accuracy of ±0.03 eV. This is accomplished by utilizing a high-precision voltage calibrator to establish the potential difference between the terminals, and hence the energy-loss scale.

The design of the apparatus is such that only the extreme forward-scattered particles are detected. The maximum scattering angle is determined by the geometry of the scattering chamber. For this study, two scattering chambers were used. One consists of a chamber 6.31 cm long defined by 0.051-cm-diam orifices. This chamber is the same as that used in all previous publications.[17–21] The second chamber has recently been completed for use in studies of doubly differential (angle and energy-loss) scattering cross sections. It consists of a chamber 1.0 cm long defined by 0.025 $\times$0.025-cm orifices. The incident angle of the beam is defined by the entrance aperture of the scattering chamber and an identical aperture located 20.0 cm in front of the entrance aperture to the scattering chamber. Similarly, the exit angle is defined by the exit aperture of the scattering chamber and another 0.025$\times$0.025-cm aperture located 25.0 cm behind the exit aperture of the scattering chamber.

If we assume a parallel beam incident upon the scattering chamber, the maximum scattering angle is 8.1×10^{-3} rad in the case of the first scattering chamber, and 1.3×10^{-3} rad for the second. The true maximum scattering angle is, of course, modified by the acceptance angle subtended at the scattering center by the detection apparatus. Geometrically, this angle is defined by the analyzer entrance slit located at the exit of the deceleration column. This slit is horizontal with a vertical width of 0.005 cm. This yields a maximum exit scattering angle of 1.6×10^{-5} rad, which is much smaller than that defined by either of the scattering chambers. However, the geometric acceptance angle of the analyzer represents an absolute lower limit on the angle of scatter. In actual practice, the ion optics of the decelerator column tend to focus the scattered beam onto the analyzer slit. Experimentally,[22] it has been shown that this focusing results in a compression of the beam by a factor of about 5 over that predicted by the assumption of straight-line trajectories. If we use this

experimental relation, we calculate the minimum acceptance angle of the detector to be approximately 1×10^{-4} rad. The actual scattering angle is somewhat larger due to the presence of nonparallel components in the incident beam. Experiment has shown that, with no gas in the scattering chamber, the transmitted intensity is one-half the peak value at an angle of $\pm5\times10^{-4}$ rad.

Previous experimental results[23] have shown that heavy-particle scattering is confined predominately to the forward direction in the energy range of the present experiment. However, in the case of neon, the results of Coffey *et al.*[3] have indicated that, at low velocities of approach, angular scattering becomes appreciable, to the extent that there is almost no forward scattering. Since the velocity at which the dominant excitation mechanism ceases to be due to molecular curve crossings is not well known, the cross sections reported here should not be considered, in the lower-velocity limit, total excitation cross sections. Rather, they should be viewed as cross sections for inelastic scattering in the forward direction integrated over an acceptance angle of $\pm5\times10^{-4}$ rad in the polar angle and over an acceptance angle of $\pm1.3\times10^{-3}$ rad in the azimuthal angle. At impact energies above 50 keV for protons, the data of Barat and Houver[23] indicate that the results may be considered to be essentially equivalent to the doubly differential cross section integrated over all angles.

The mathematical details by which cross sections may be extracted from the data have been discussed in detail by Schoonover and Park[20] and by Schoonover.[24] Basically, the analysis may be expressed in terms of differential equations relating the loss and gain terms of various partial beams. Exact solution of these differential equations yields the detectable current due to the transition, $(I_{1a})_f$, in terms of the detected zero-energy-loss component $(I_{10})_f$. That is,

$$(I_{1a})_f = nl\sigma_a(I_{10})_f \quad , \tag{1}$$

where l is the effective scattering length, n is the number density of scatterers, and σ_a is the cross section for excitation with scattering within the acceptance angle. Since the apparatus has a finite energy resolution, the actual detected current is a convolution of the dispersive effects of the apparatus with the initial energy spread of the beam and the effects of the target gas. That is, the detected energy-loss spectrum $R(\xi)$ as a function of the energy loss ξ can be written as

$$R(\xi) = nl\int \Phi(\xi-\xi')\frac{d\bar{\sigma}(\xi')}{d\xi}\,d\xi'. \tag{2}$$

The energy-loss spectrum generated with no target gas in the scattering chamber $\Phi(\xi)$, is itself a convolution of the dispersive effects of the apparatus with the initial energy spread of the beam. $d\bar{\sigma}/d\xi$ is the doubly differential cross section integrated over the instrument acceptance angles. n and l are as defined previously. Then the experimental equation for determination of σ_a becomes

$$\sigma_a = \frac{1}{nl}\left(\frac{\int_{\Delta\xi_a} R(\xi)\,d\xi}{\int_{\Delta\xi_0} R(\xi)\,d\xi} - \frac{\int_{\Delta\xi_a}\Phi(\xi)\,d\xi}{\int_{\Delta\xi_0}\Phi(\xi)\,d\xi}\right). \tag{3}$$

The integration limits $\Delta\xi_a$ and $\Delta\xi_0$ are the energy-loss intervals over which the spectrum is nonzero for the transition and monoenergetic beams, respectively. Application of this equation implicitly assumes that the spectrum drops essentially to zero on both sides of the transition peak. That is, the energy loss associated with the transition must be sufficiently remote from neighboring processes that the finite resolution of the apparatus does not introduce contributions from these nearby processes to the peak under evaluation.

All data were obtained in the form of energy-loss–current data pairs punched on paper tape. The required integrals were then obtained numerically by application of Simpson's rule using a small digital computer. All data were obtained at target thicknesses for which $(I_{1a})_f/(I_{10})_f$ was a linear function of target particle density, that is, under single-collision conditions.

III. ENERGY-LOSS SPECTRA

Typical energy-loss spectra obtained for heavy-ion impact on neon are shown in Fig. 1 for the three ionic projectiles used in this study. The data shown are unretouched computer plots of the apparent differential cross section as a function of energy loss. The term apparent here means that the instrumental resolution function has not yet been unfolded from the experimental results. However, all other experimental parameters have been removed in accordance with the differential form of Eq. (1). The three peaks observed correspond, in order of increasing energy loss, to the $(2p^5)3s$, $3p$, and $4s$ configurations of neon.

The level structure within these configurations is shown in Fig. 2. The data presented are taken from the tables of Moore.[25] The energy-level structure is shown to scale on the extreme left. The energy scales are then expanded for the $(2p^5)3s$ and $(2p^5)3p$ configurations in order to show the detail. The appropriate LS- and jj-term values, as well as the Paschen notation, are listed for each level in the center of the figure. Several important optically allowed transitions are shown. Those allowed under assumptions of LS coupling are shown in the left-hand column, while those allowed under assumptions of jj coupling are shown in the right-hand column.

The formalism which has been developed for describing the coupling in two-electron spectra can be carried over to neon (and the other rare gases) if we use the angular momenta of the unfilled p shell in place of that of the inner electron. This formalism has been described in detail by Cowan and Andrew.[26] For the lower excited states of neon, LS coupling is assumed to be valid. As the outer electron is promoted to high excited states, the levels are observed to occur in pairs. This intermediate-pair structure leads to a description of the coupling intermediate between pure LS and pure jj, which is called jK coupling. Now the spin-orbit coupling of the core becomes the dominant interaction, with the electrostatic interaction becoming the second most important one. In this case, the total orbital angular momentum and spin angular momentum are no longer good quantum numbers. In all cases, however, J is a good quantum number and the actual wave functions for any state of intermediate coupling can be expressed in terms of a linear combination of basis functions for any of the pure-coupling cases. Thus, the wave functions for the $3s$ configuration can be written as combinations of the LS basis functions:

$$
\begin{aligned}
\Psi(1s_2) &= \alpha\phi(^1P_1) + \beta\,\phi(^3P_1),\\
\Psi(1s_3) &= \phi(^3P_0),\\
\Psi(1s_4) &= -\,\beta\phi(^1P_1) + \alpha\phi(^3P_1),\\
\Psi(1s_5) &= \phi(^3P_2).
\end{aligned}
\tag{4}
$$

The notation on the left-hand side is the Paschen notation with the subscript increasing with decreasing energy. We note that mixing only occurs for levels with the same value of J and that the $1s_3$ and $1s_5$ levels remain pure triplets. For neon, the coefficients[27] are $\alpha = 0.964$ and $\beta = 0.266$ yielding an LS purity of 93% for the $(2p^5)3s$ configuration.

A test of the coupling is provided by heavy-particle impact. For proton impact, transitions involving a change in multiplicity are expected to be forbidden since this would constitute a violation of the Wigner spin-conservation rule.[28] In essence, this rule states that the total spin of the colliding system must be conserved in the collision. The rule is expected to be rigorous when the spin-orbit interaction is small, i.e., under conditions of good LS coupling. The rule has been experimentally verified for proton impact upon helium.[29–31] When the spin-orbit interaction becomes large, however, the total spin no longer remains a good quantum number. In that case, the Wigner spin rule loses rigor and proton-impact excitation of "triplet" states is allowed. For impact by electrons or heavy particles which carry an electron, excitation can take place by electron exchange; hence, both triplet and singlet states may be excited regardless of the type of coupling.

While the separations of the levels within the $(2p^5)3s$ configuration are much too small to be resolved by the energy-loss spectrometer, an appreciable contribution due to excitation of the triplet levels should produce a detectable shift in the energy-loss location of the peak corresponding to the $3s$ configuration.

We have made a systematic study of the energy loss associated with the $3s$ peak as a function of ion type and impact energy. The results indicate that for protons the energy-loss location is 16.83 eV over the entire range of impact energies. For H_2^+ impact, the location is 16.74 eV for 30-keV particles but rapidly increases to 16.83 eV for 60-keV particles. The energy-loss location remains fixed over the remainder of the energy range. For helium ions, however, the energy loss is 16.74 eV for 20-keV particles and very slowly increases to 16.83 eV for 170-keV particles. The energy shifts to higher values monotonically with increasing impact energy.

To a large extent the $1s_2$ level at 16.85 eV, which is predominately singlet in nature, is populated by H_2^+ and He^+ impact at the high impact energies; the remaining $1s_3$, $1s_4$, and $1s_5$ levels, which are pre-

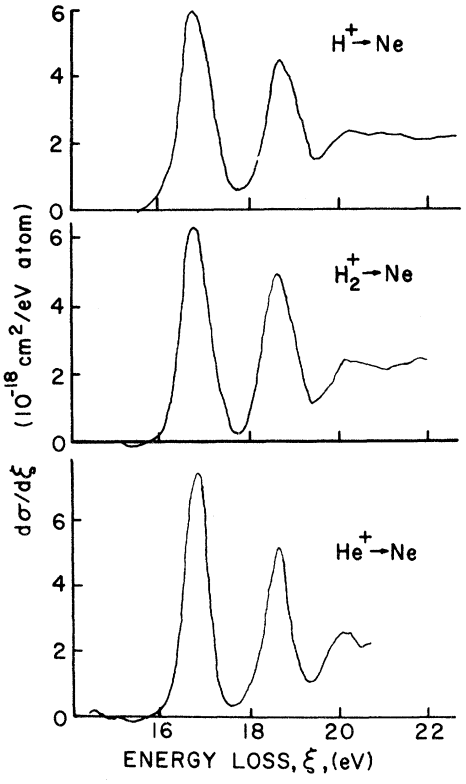

FIG. 1. Typical apparent differential energy-loss cross sections. The data shown are unretouched computer plots for each of the three ions used in this study. The impact velocity in all cases is 2.76×10^8 cm/sec.

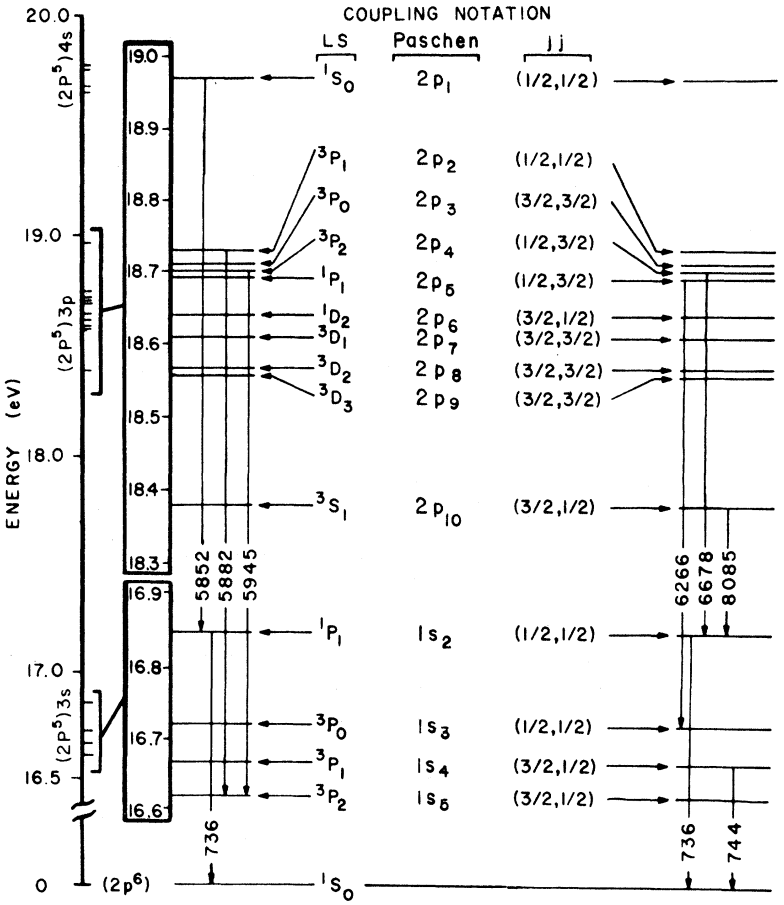

FIG. 2. Energy-level diagram of neon. The data are taken from Moore (Ref. 25). The structure is shown to scale on the extreme left. The scale is then expanded to the right to show the detail of the $(2p^5)3s$ and $(2p^5)3p$ configurations. Appropriate *LS* and *jj* term designations are listed in the center, and important optically allowed transitions under assumptions of *LS* coupling are shown on the left-hand side, while those allowed under assumptions of *jj* coupling are shown on the right-hand side. All transition wavelengths are in angstroms.

dominately triplet and are bunched at 16.67 eV, seem to be excited in addition to the $1s_2$ level at low energies by H_2^+ and He^+ impact. Excitation by H^+ impact is predominately to the $1s_2$ level for all impact energies. In light of the Wigner spin conservation rule, which predicts only singlet-state excitation by H^+ but allows triplet-state excitation by the electron bearing H_2^+ and He^+ in resonant conditions (narrow range of low energies), the *LS*-coupling scheme appears to yield a good description of the $(2p^5)3s$ levels of the neon atom. This is in agreement with the results obtained theoretically by Fajen and co-workers[5,27] as mentioned earlier.

A curve-fitting technique has been developed to express the results described above in a more quantitative manner. The information obtained by this method is described in Sec. V.

IV. DATA

In this section, data are presented for excitation of the sum of levels in the $(2p^5)3s$ and $(2p^5)3p$ electronic configurations of neon. The error bars in all cases represent a vectorial (rms) addition of one standard deviation and of an estimated 10% systematic error, largely due to uncertainties in the pressure measurements. Each datum point represents approximately 20 data trials.

A. 3s Configuration

The results obtained for proton-impact excitation of the 3*s* configuration are shown in Fig. 3(a). These results were obtained using the second scattering chamber discussed in Sec. II. The angular spread of the incident beam is smaller for this chamber than that of the original scattering chamber. However, the results agree, within experimental error, with a previous set of preliminary data taken with the original scattering chamber.[32]

There are no previous experimental results for excitation of this level with which to compare our results. The only previous work for proton impact in this energy range are those of de Heer and co-workers[6,7] van Eck *et al.*,[8] and Jaecks *et al.*[9] They did not measure excitation cross sections directly, but measured optical emission cross sections by detection of the radiation from the subsequent decay of the excited neon target. Such cross sections can be converted to level-excitation cross

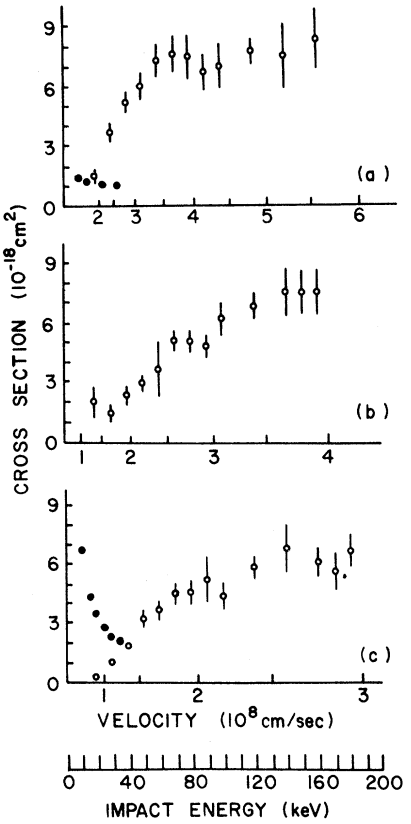

FIG. 3. Absolute cross section for excitation of the $(2p^5)3s$ configuration of neon as a function of impact velocity. (a) H^+ impact; (b) H_2^+ impact; (c) He^+ impact. The open circles are present data; in (a) the closed circles are the emission cross-section data of de Heer *et al.* (Ref. 6); in (c) the closed circles are the emission cross sections of de Heer and co-workers (Refs. 6 and 7) and of van Eck *et al.* (Ref. 8).

sections provided one knows the appropriate transition probabilities and emission cross sections for higher-lying states. The recent work of Bridges and Wiese[33] has provided accurate transition probabilities for the $3p$ levels of neon. However, all of the necessary emission cross sections have not been measured and no attempt was made, therefore, to convert the emission data to level-excitation cross sections. To provide a comparison, however, the emission data of de Heer *et al.*,[6] which consist of the sum of emission cross sections for the $1s_2$ and $1s_4$ lines, are also shown in Fig. 3(a).

Agreement is not good, neither in shape nor in absolute magnitude. The discrepancy in magnitude is not surprising, both in view of the differences in measured quantities and in view of the inherent difficulties of the optical method for this level. Emission from the $3s$ level lies in the vacuum ultraviolet where standard sources are not available for calibration purposes.

The difference in shape is somewhat surprising, however. The decrease in our data at lower energies compared to the emission results could be due to enhancement of scattering to angles greater than our acceptance angle. There is no explanation at present, though, for the region in which our data are higher. All systematic errors associated with the present method, such as loss due to scattering, would tend to make our cross sections too low. In addition, the crossover cannot be attributed to the differences in measured quantities since, for this level, the only difference between emission and excitation cross sections can be cascade contributions from higher levels, which would tend to make the emission data higher than the excitation data.

The data for excitation by H_2^+ and He^+ are shown in Figs. 3(b) and (c), respectively. Both ions show the same behavior with impact velocity as that observed for protons. In both cases, the onset is slightly less rapid than for protons, and the maximum value obtained by He^+ is slightly smaller. There are no other data available for comparison with our H_2^+ data. The small increase in the cross section at 20 keV appears to be real. Experimental difficulties prevented extension of the data to lower energies to see if another process is becoming dominant. It should be noted here that the cross sections reported here for H_2^+ are for excitation without simultaneous dissociation of the projectile. Excitations which occur with dissociation are not observable with the present apparatus.

The emission cross-section data of de Heer and coworkers[6,7] and of van Eck *et al.*[8] are shown for comparison with our He^+ data in Fig. 3(c). The discrepancy in shape noted in the case of proton impact is much more pronounced for He^+ impact. The increase in cross section with decreasing impact energy for this system has also been observed by Coffey *et al.*[3] and Liples *et al.*[1] for very low impact energy (< 1 keV). It is possible that the formation of quasimolecular states is becoming important at the lower velocities of our experiment, with resultant scattering at large angles.

B. $3p$ Configuration

The results obtained for ionic impact excitation of the $(2p^5)3p$ electronic configuration of neon are shown in Figs. 4(a)–(c) for H^+, H_2^+, and He^+ impact, respectively. All levels of this configuration are optically forbidden from the ground state by parity selection rules (Δl of the excited electron is zero).

All of the data exhibit nearly identical behavior. In all cases, the slopes of the onset, as functions of impact velocity, are very nearly identical within the experimental error. In addition, the cross section in each case reaches a maximum value of

$\approx 4.5\times10^{-18}$ cm^2 at an impact velocity of $\approx 3\times10^8$ cm/sec.

Since these transitions are optically forbidden, one expects, from qualitative results obtained by the Born approximation, that the high-energy fall-off in the cross section should be very rapid ($\propto 1/E$). In the case of proton impact, our data indicate this type of behavior. For H_2^+ impact, the cross section is definitely decreasing above 90 keV. We were not able to observe the phenomenon for He^+ impact since our highest energy lies just above the peak of the curve.

For H^+ and He^+, emission cross-section data of de Heer and co-workers,[6] of van Eck *et al.*,[8] and of Jaecks *et al.*[9] are shown for comparison with our results. Their data consist of the sum of three transitions from levels with the $3p$ configuration to levels of the $3s$ configuration having wavelengths of 5852, 5882, and 5945 Å. The agreement between proton data is surprisingly good in view of the fact that only three of the many possible deexcitation channels are included and since no corrections for cascade effects have been made to the emission data. It is not known if the agreement observed is merely fortuitous, or if the major deexcitation channels are indeed these three. The data of Sharpton *et al.*[5] would seem to imply that the latter is the case.

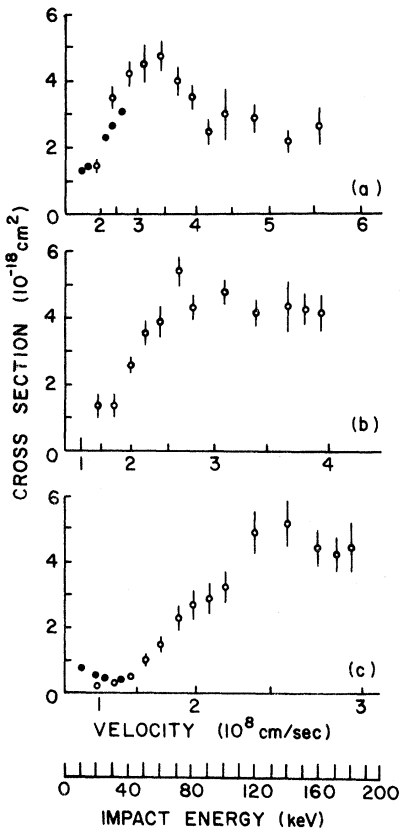

FIG. 4. Absolute cross section for excitation of the $(2p^5)3p$ configuration of neon as a function of impact velocity. (a) H^+ impact; (b) H_2^+ impact; (c) He^+ impact. The open circles are present data; the closed circles are the emission cross-section data of de Heer *et al.* (Ref. 6), van Eck *et al.* (Ref. 8), and Jaecks *et al.* (Ref. 9).

The agreement between He^+- impact data is not as good, but within the combined experimental errors. Again, since previous experiments have indicated increasing cross sections with decreasing energy for the He^+-Ne system, it is reasonable to assume that excitation of this configuration may also be resulting in large-angle scatter at low energy.

V. CURVE FITTING OF $(2p^5)3s$ PEAK

As previously mentioned in Sec. III, analysis of the energy-loss location of the $(2p^5)3s$ peak as a function of both incident ion and impact energy yielded an indication of the excitation of the $1s_3$, $1s_4$, and $1s_5$ states which have triplet characteristics for H_2^+ and He^+ impact at low energy. The results of that analysis were necessarily of a qualitative nature. In an attempt to express our results in a more quantitative manner, we have developed a curve-fitting technique to extract unresolved cross sections from our experimental data. The technique has been used previously with reasonable success for analysis of helium excitations as observed in He^+-He scattering.[34]

The method is described in detail elsewhere[16] and only a brief description of the essential elements will be given here. Basically, successful application of the technique rests on four assumptions:

(i) The energies of discrete excitations are assumed to be located at the spectroscopically determined energy values.

(ii) The shape of the response of each excitation is identical to that of the elastically transmitted peak or the resolution function.

(iii) The energy-loss spectral response of one excitation is unaffected by the responses of neighboring excitations, with the total response being simply additive for coincident excitations.

(iv) All of the energy-loss processes which contribute to the unresolved peak are known.

All of the above assumptions are valid for our particular experiment. Assumptions (ii) and (iii) have been discussed in detail elsewhere.[24] Under these assumptions, then, each point of the inelastic energy-loss spectrum can be written

$$R(\xi_i) = nlR_e(\xi=0)\sum_{j=1}^{n}\sigma_j\left(\frac{\kappa_e(\xi_i-\xi_j)}{R_e(\xi=0)}\right) \quad , \qquad (5)$$

where $R(\xi_i)$ is a discrete point on the inelastic energy-loss spectrum located at an energy loss ξ_i;

$R_e(\xi_i - \xi_j)$ is the resolution function evaluated at $(\xi_i - \xi_j)$, where ξ_j is the energy-loss location of transition j having a cross section σ_j; n and l are as defined previously. The sum is taken over all transitions which have energy losses lying within the resolution width of ξ_i. Of course this particular equation assumes discrete processes and thus is valid only to energy losses which lie greater than the resolution half-width below the onset of the ionization continuum.

In principle, if n discrete processes contribute to an unresolved peak, then only n points on the spectrum are required for a unique solution of Eq. (5). However, due to unavoidable random noise in the data, the accuracy of an exact solution is somewhat in doubt. Thus, to improve the accuracy, the equation is least-squares fitted to k points on the energy-loss spectrum, where k is taken as large as possible without including contributions from processes not considered in the sum over j. (Typically, k was chosen to be 20 for present measurements.) The cross sections are then obtained as the least-squares parameters of the equation and the calculated error in the parameters gives a reasonable estimate of the goodness of fit.

The technique was applied to the 3s peak in neon by assuming peaks at the spectroscopic locations of the four levels in the configuration (see Fig. 2). For this case, a fit to these four levels yielded results which, due to their extremely small separations and due to inherent noise in the data, possessed rather large statistical fluctuations for the three lower (triplet) levels. Therefore, the results reported here are for the sum of the triplet levels as this number was statistically more significant. In addition, approximately the same values were obtained by making another approximation and fitting a two-parameter equation with peaks at 16.85 eV ($1s_2$) and the symmetric center of the triplets at 16.67 eV ($1s_4$). Unfortunately this restricts interpretation of the results since this level is also the one which could be populated directly if neon was not describable by LS coupling for this configuration. However, the individual triplet cross sections cannot be expected to be statistically significant in this experiment since their energy separation approaches the energy-loss uncertainty of ±0.03 eV.

The results of the least-squares analysis provided a fit to better than 5% of the larger contribution in all cases. The results are presented in Figs. 5–7 for H^+, H_2^+, and He^+, respectively.

Each datum point consists of approximately 12 data trials. The parameters obtained from the curve fitting for each of the trials were used to obtain a weighted average, the weight factors being the relative inverse of the calculated errors in the parameters. The error bars in all cases represent an rms combination of one standard deviation obtained from the averaging procedure, together with an additional uncertainty of 25%. This 25% arises from uncertainties involved in the curve-fitting procedure and does not apply to the cross section for the sum of the levels.

Very little triplet excitation is observed for proton and H_2^+ impact. The maximum value for proton impact is of the order of 25% of the total excitation cross section. This is slightly larger than what would be expected by application of the Wigner spin rule. A crude comparison can be made between our data and the coefficient calculated by Fajen[27] for the singlet-triplet mixing in this configuration.

Using the first Born approximation, we can calculate the relative direct (nonexchange) population of the 16.67-eV level ($1s_4$) due to mixing within

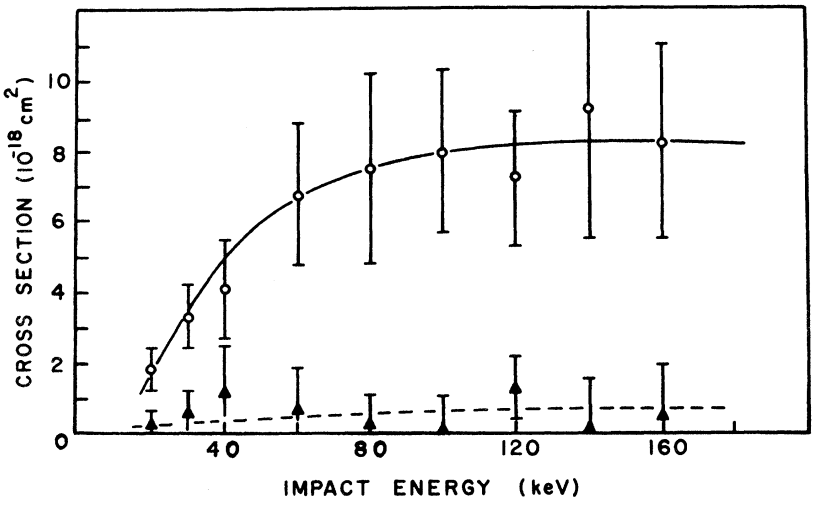

FIG. 5. Cross sections for excitation of the singlet and triplet levels within the $(2p^5)3s$ configuration by H^+ impact. The open circles are data for excitation of the $1s_2$ level. The solid triangles are data for excitation of the sum of the triplet levels. The dashed line is our calculated estimate of the direct population of the $1s_4$ level due to intermediate coupling.

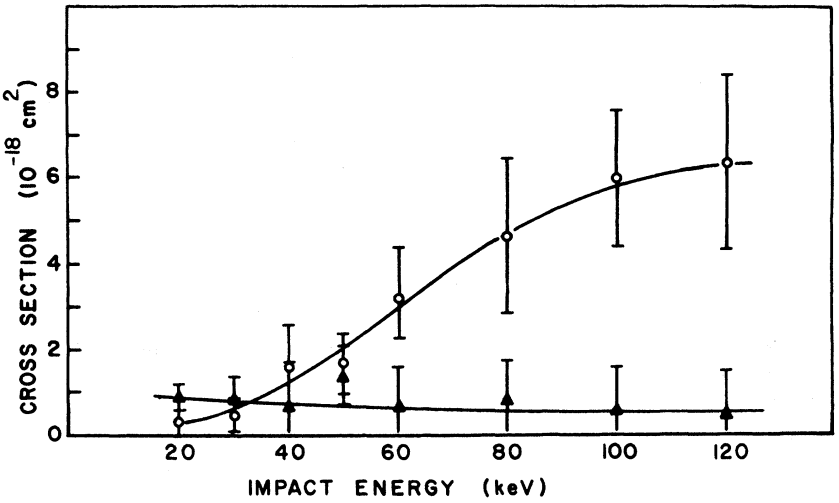

FIG. 6. Cross sections for excitation of the singlet and triplet levels within the $(2p^5)3s$ configuration by H_2^+ impact. The open circles are data for excitation of the $1s_2$ level. The solid triangles are data for excitation of the sum of the triplet levels.

the one-configuration approximation. We find that

$$\sigma'_{0n} \simeq (\beta^2/\alpha^2)\sigma_{0n} \quad , \tag{6}$$

where σ'_{0n} is the cross section for direct excitation of the $1s_4$ (triplet) level and σ_{0n} is the cross section for excitation of the $1s_2$ level. β and α are the coupling coefficients defined previously. Using the calculated results of Fajen,[27] the cross section for direct population of the $1s_4$ (triplet) level should be

$$\sigma'_{0n} \simeq 0.76\sigma_{0n} \quad . \tag{7}$$

This relation has been applied to our data to calculate a cross-section curve for excitation of the $1s_4$ level, which is plotted in Fig. 5. Agreement is remarkably good at energies above 80 keV. In the range from 20–80 keV, our data show a slightly higher cross section with a peaked structure. However, within the error of the measurement and the calculation, it is impossible to make any definite statements.

The lack of triplet excitation by H_2^+ is surprising. Since this ion carries an electron, excitation of triplet levels should occur by electron exchange. One is tempted to conclude that exchange excitation does not occur very significantly for H_2^+ bombardment. However, van den Bos *et al.*[35] and Rudd[29] have observed triplet excitation of helium by H_2^+ impact, with cross sections comparable to those for excitation for the singlet states. A possible explanation for this apparent discrepancy is that sufficient distortion of the molecular structure occurs during the collision that the H_2 ion dissociates. Our experiment would not detect such a result since analysis is done on the primary particle. The experiment of van den Bos *et al.* would not be sensitive to this process either, since only the optical emission is studied, while all of the

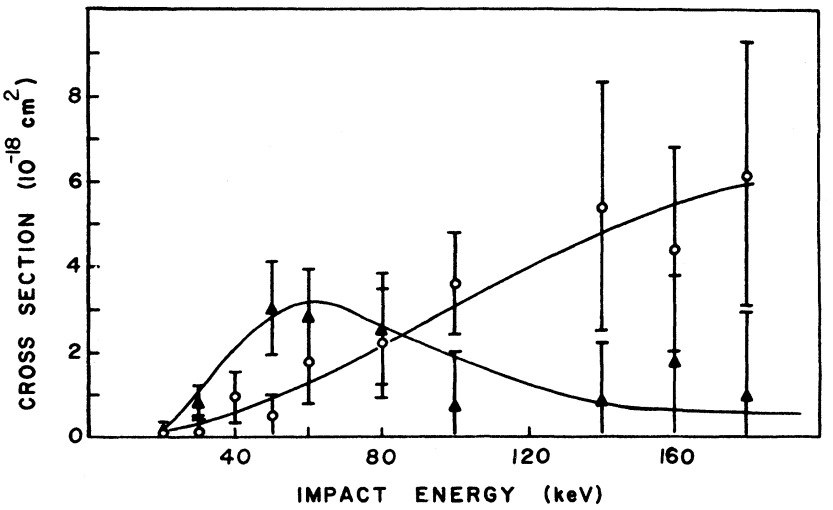

FIG. 7. Cross sections for excitation of the singlet and triplet levels within the $(2p^5)3s$ configuration by He^+ impact. The open circles are data for excitation of the $1s_2$ level. The solid triangles are data for excitation of the sum of the triplet levels.

incident beam is collected in a Faraday cup, without mass analysis.

Helium-ion impact thus provided the only data in which significant triplet excitation occurred. To the authors' knowledge, there are no other experimental data with which to compare these results.

VI. DISCUSSION

At present, the authors know of no theoretical calculations for this system with which to compare present results. The data presented here are the first excitation measurements using the technique of heavy-ion energy-loss spectrometry for which data obtained by the optical method have been available for comparison. Agreement is not good for excitation of the $(2p^5)3s$ configuration. Part of the discrepancy may be explainable by the differences in the measured quantities, and the absolute numbers (except for the case of He^+ impact at very low energies) are within the combined errors of the two methods. The differences in shape are disturbing, however. Resolution of this problem must await a more detailed analysis of the cross-section function as a function of scattering angle. Agreement between data for the excitation of the $(2p^5)3p$ configuration was surprisingly good.

Analysis of the relative population of singlet-triplet levels within the $3s$ configuration, while yielding values with relatively large experimental uncertainties, has been able to illustrate some qualitative aspects of the heavy-ion–neon scattering process. The proton-impact data are in agreement with both the Wigner spin rule and the calculated LS purity of the $3s$ configuration, as expected. The He^+ data indicate that triplet excitation by electron exchange is a significant process in neon at low velocities and cannot be excluded from any theoretical attempts to explain scattering phenomena in the energy range of the present experiment.

The data for triplet excitation by H_2^+, together with the data of Rudd[29] and van den Bos *et al.*,[35] could imply that electron exchange occurs only with concurrent dissociation of the H_2^+ molecule. Further experimental investigation of this system by actually measuring cross sections for simultaneous electron exchange dissociation is suggested and should yield interesting information.

---

†Work supported by a grant from the National Science Foundation.

*Present address: JILA, University of Colorado, Boulder, Colo. 80302.

[1]M. Liples, R. Novick, and N. H. Tolk, Phys. Rev. Letters 15, 815 (1965).

[2]J. Baudon, M. Barat, and M. Abignoli, J. Phys. B 3, 207 (1970).

[3]D. Coffey, D. C. Lorents, and F. T. Smith, Phys. Rev. 187, 201 (1969).

[4]C. E. Brion and L. A. R. Olson, J. Phys. B 3, 1020 (1970).

[5]F. A. Sharpton, R. M. St. John, C. C. Lin, and F. E. Fajen, Phys. Rev. A 2, 1305 (1970).

[6]F. J. de Heer and J. van Eck, in *Proceedings of Third International Conference on the Physics of Electronic and Atomic Collisions, London* (North-Holland, Amsterdam, 1963), pp. 635–643.

[7]F. J. de Heer, B. F. J. Luyken, D. Jaecks, and L. Wolterbeek Muller, Physica 41, 588 (1969).

[8]J. van Eck, F. J. de Heer, and J. Kistemaker, Phys. Rev. 130, 656 (1963).

[9]D. Jaecks, F. J. de Heer, and A. Salop, Physica 36, 606 (1967).

[10]E. W. Thomas and H. B. Gilbody, Proc. Phys. Soc. (London) 85, 363 (1965).

[11]J. T. Park and F. D. Schowengerdt, Rev. Sci. Instr. 40, 753 (1969).

[12]R. K. Goodman and A. L. Hunt, Bull. Am. Phys. Soc. 15, 1442 (1970).

[13]E. U. Condon and G. H. Shortley, *The Theory of Atomic Spectra* (Cambridge U. P., Cambridge, 1935), p. 301.

[14]Colutron Corp., Boulder, Colo. 80302.

[15]MKS Instruments, Inc., Burlington, Mass.

[16]G. W. York, Jr., Ph. D. dissertation (University of Missouri-Rolla, 1971) (unpublished); see also, G. W. York, Jr., J. J. Miskinis, J. T. Park, D. H. Crandall, and V. Pol., Rev. Sci. Instr. 43, 230 (1972).

[17]J. T. Park and F. D. Schowengerdt, Phys. Rev. 185, 152 (1969).

[18]F. D. Schowengerdt and J. T. Park, Phys. Rev. A 1, 848 (1970).

[19]J. T. Park, D. R. Schoonover, and G. W. York, Phys. Rev. A 2, 2304 (1970).

[20]D. R. Schoonover and J. T. Park., Phys. Rev. A 3, 228 (1971).

[21]J. T. Park, F. D. Schowengerdt, and D. R. Schoonover, Phys. Rev. A 3, 679 (1971).

[22]F. D. Schowengerdt, Ph. D. dissertation (University of Missouri-Rolla, 1969) (unpublished).

[23]M. Barat and J. C. Houver, Compt. Rend. 264B, 38 (1967); 264B, 296 (1967).

[24]D. R. Schoonover, Ph. D. dissertation (University of Missouri-Rolla, 1970) (unpublished).

[25]C. E. Moore, *Atomic Energy Levels*, Natl. Bur. Std. (U.S.) Circ. No. 467 (U.S. GPO, Washington, D.C., 1949).

[26]R. D. Cowan and K. L. Andrew, J. Opt. Soc. Am. 55, 502 (1965).

[27]F. E. Fajen (private communication).

[28]For a discussion of Wigner's rule, see J. B. Hasted, *The Physics of Atomic Collisions* (Butterworth, Washington, 1964), p. 327.

[29]M. E. Rudd, Phys. Rev. Letters 15, 580 (1965).

[30]J. van den Bos, G. J. Winter, and F. J. de Heer, Physica 40, 357 (1968).

[31]H. S. W. Massey and E. H. S. Burhop, in *Electronic and Ionic Impact Phenomena* (Clarendon, Oxford, 1952), p. 63.

[32]J. T. Park and G. W. York, Bull. Am. Phys. Soc. 15, 1503 (1970).
[33]J. D. Bridges and W. L. Wiese, Phys. Rev. A 2, 285 (1070).
[34]D. R. Schoonover and J. T. Park, in *Proceedings of the Seventh International Conference on the Physics of Electronic and Atomic Collisions, Amsterdam* (North-Holland, Amsterdam, 1971), p. 839.
[35]J. van den Bos, G. J. Winter, and F. J. de Heer, Physica 44, 143 (1969).

PHYSICAL REVIEW A VOLUME 6, NUMBER 4 OCTOBER 1972

Ionization Cross Sections of Gaseous Atoms and Molecules for High-Energy Electrons and Positrons*

Foster F. Rieke† and William Prepejchal
Argonne National Laboratory, Argonne, Illinois 60439
(Received 31 May 1972)

Ionization cross sections of forty gases have been measured for electrons of kinetic energies 0.1–2.7 MeV. The measurements are absolute and extensive precautions have been taken to minimize systematic and accidental errors. The energy dependence of the measured cross sections is accurately described by the Bethe asymptotic formula involving two parameters that represent important atomic properties. Comparisons have been made between H_2 and D_2 and between CH_4 and CD_4; the observed differences are of the order of 1% and too small to be resolved with certainty. A close comparison has been made between positrons and electrons in Ar at 0.67 and 1.1 MeV; the cross sections are observed to be equal within a probable error of 0.5%.

I. INTRODUCTION

Although primary ionization cross sections[1] for high-energy (MeV) electrons are of practical importance and have a behavior that theoretically is simple and well understood, very few absolute values have been available from either experiment or theory. The earliest measurements[2,3] consisted in counting primary ionization events along cloud-chamber tracks. The method we have employed is based on the determination of the efficiency of a gas-filled counter in responding to monoenergetic β rays. That method was first used by Graf[4] in measurements of air and later by McClure,[5] who made measurements of H_2, He, Ne, and Ar over the energy range 0.2–1.6 MeV. Elaborating upon McClure's experiments, we have constructed an improved apparatus and studied a larger variety of gases over a somewhat wider range of energies. Throughout, we have endeavored to minimize systematic errors. The present paper is a comprehensive summary of our work, which has been described in part in the form of preliminary reports.[6–9]

To systematize the results, the Bethe theory[10–13] is employed. McClure found (and we have confirmed) that for each gas the measured cross sections are described accurately by the following relation, which he extracted from the Bethe theory,

$$\sigma = Ax_1 + Bx_2, \tag{1}$$

where

$$x_1 = \beta^{-2}\ln[\beta^2/(1-\beta^2)] - 1, \quad x_2 = \beta^{-2},$$

β = (velocity or primary electron)/(velocity of light), and A and B are empirical constants characteristic of gas.

Bethe carried out the theory in detail, with a quantum-mechanical evaluation of the constants, for hydrogenic systems only.[10] The theoretical definition of McClure's constants A and B for the general case was given by Fano.[13] Explicit formulas and a discussion of the approximations that they involve are given also in Ref. 12. As explained in Sec. 4.1 of that reference, the cross section σ_n for a fast electron to excite a target atom (or molecule) from the ground state to a state n is given by

$$\sigma_n = 4\pi(\hbar/mc)^2 (M_n^2 x_1 + C_n x_2), \tag{2}$$

where $4\pi(\hbar/mc)^2 = 1.874\times10^{-20}$ cm^2 and M_n^2 and C_n are expressed in terms of the generalized oscillator strength for the transition involved. By summation over the appropriate transitions (integration for states in the continuum), Eq. (1) is obtained in the form

$$\sigma = 4\pi(\hbar/mc)^2 (M^2 x_1 + C x_2), \tag{3}$$

which we shall use in reporting our results.

The quantity M^2 may be called the total dipole-matrix element squared for ionization, measured in units of $a_0^2 = (\hbar^2/me^2)^2$, the Bohr radius squared. In general, the M^2 for each atom or molecule includes contributions from different electron shells that are roughly proportional to the square of shell radii. Major contributions thus should stem from